Science Advances

www.advances.sciencemag.org/cgi/content/full/1/7/e1500229/DC1

Supplementary Materials for

Intrinsic coupling modes reveal the functional architecture of cortico-tectal networks

Iain Stitt, Edgar Galindo-Leon, Florian Pieper, Gerhard Engler, Eva Fiedler, Thomas Stieglitz, Andreas K. Engel

Published 7 August 2015, *Sci. Adv.* **1**, e1500229 (2015)
DOI: 10.1126/sciadv.1500229

This PDF file includes:

Supplemental Figures

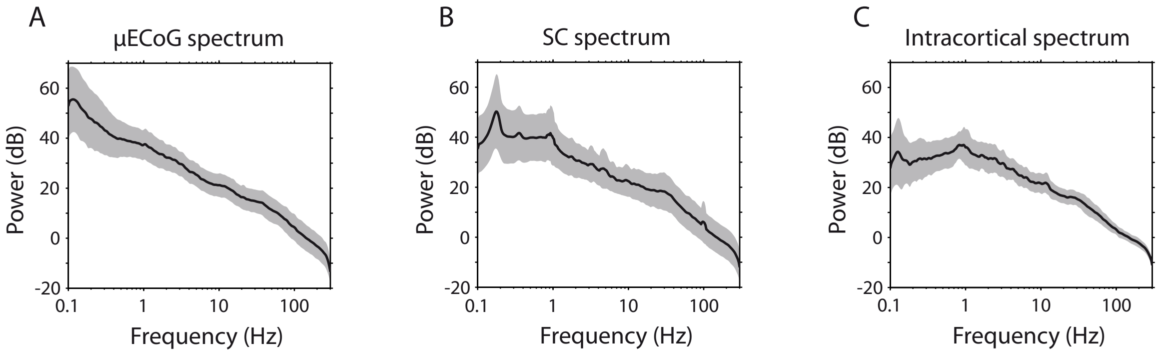

Figure S1. (**A-C**) Population average power spectra of μECoG, SC and intracortical recording sites, respectively (± standard error mean).

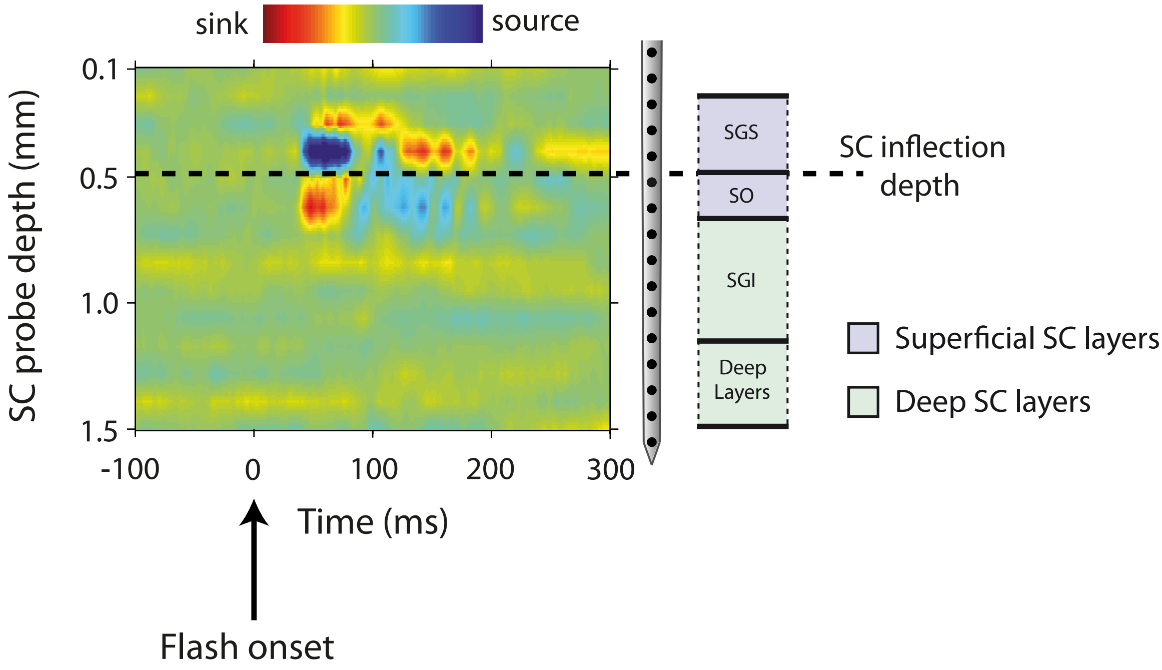

Figure S2. Recording depth in the SC was determined by current source density analysis. In a previous study *(19)*, our lab demonstrated that the border between flash-evoked current sources and sinks corresponds to the anatomical border between the two main superficial SC layers, the SGS and SO. Recording contacts were separated into two groups for depth-wise analysis, superficial SC - encompassing channels 300µm above and 200µm below the inflection depth, and deep SC - all channels situated deeper than 200µm below the inflection depth. Abbreviations: SGS – *stratum grieum superficiale*; SO – *stratum opticum*; SGI – *stratum griseum intermediale*.

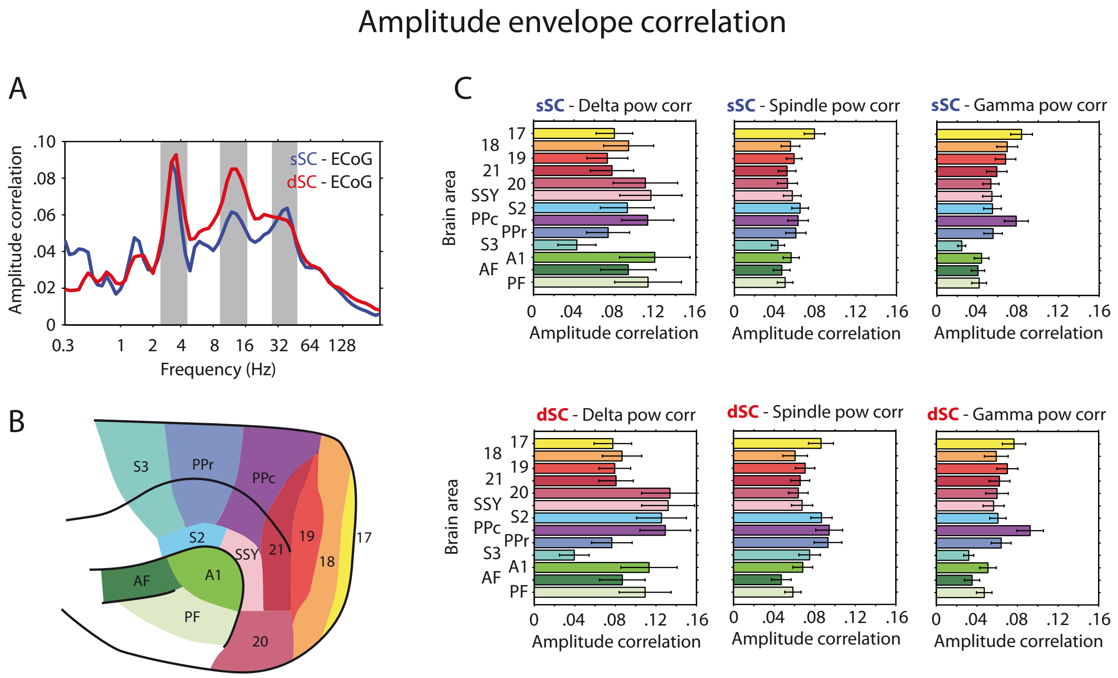

Figure S3. Large-scale structure of envelope coupling modes. (**A**) Population averaged cortico-tectal amplitude envelope correlation computed for SC recording contacts located in superficial (blue) and deep (red) SC layers. Note the peaks in cortico-tectal power correlation for delta, spindle and gamma frequencies. (**B**) Parcellation of the cortical surface into 13 different anatomically and functionally specialized regions. (**C**) Population averaged (± SEM), region-specific strength of cortico-tectal amplitude correlation the delta, spindle, and gamma frequencies identified in **A**. Superficial SC-µECoG channel pairs are plotted in the top row, with deep SC-µECoG channel pairs plotted below. Abbreviations: SSY – suprasylvian area; PPc – posterior parietal caudal area; PPr – posterior parietal rostral area; S2 – second somatosensory area; S3 – third somatosensory area; A1 – primary auditory cortex; AF – anterior auditory areas; PF – posterior auditory areas.

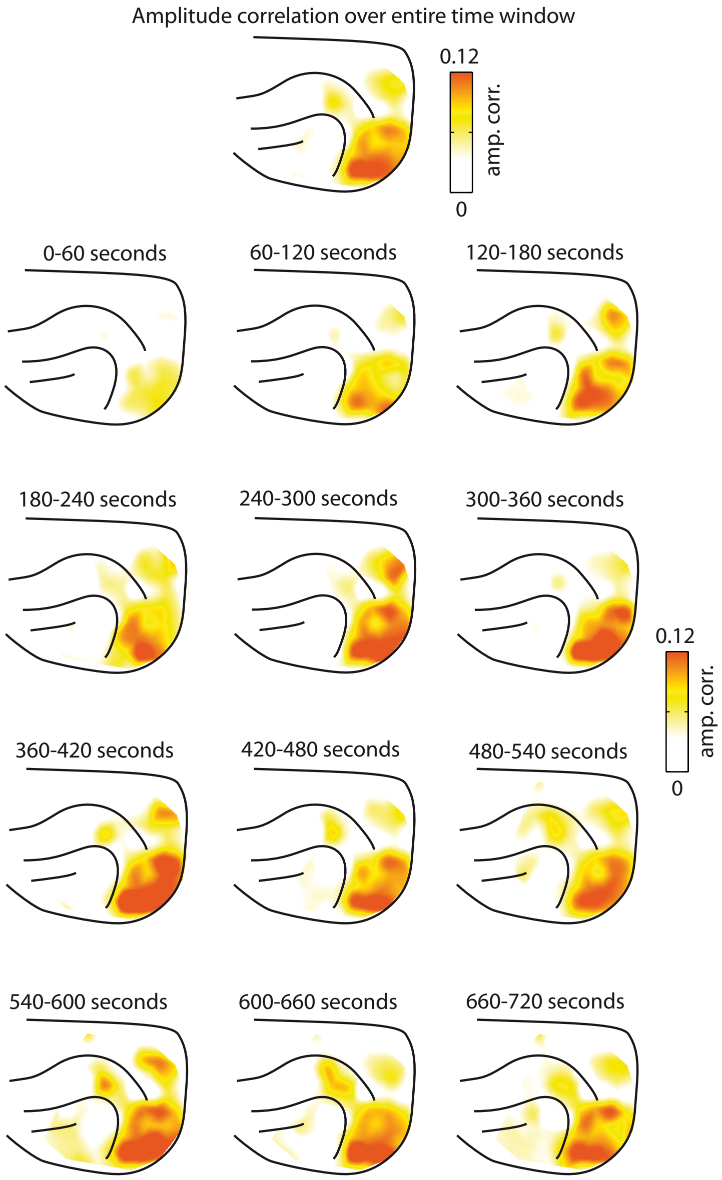

Figure S4. Temporal variability of cortico-tectal high frequency amplitude envelope correlation. (**A**) Example cortical topography of SC-μECoG amplitude correlation computed over approximately 12 minutes of data. (**B**) Strength of cortico-tectal amplitude correlation for the same example displayed in **A**, with correlation computed for 12 separate non-overlapping one-minute blocks. Note that the strength of amplitude correlation displays variation over time, however the topography remains constant.

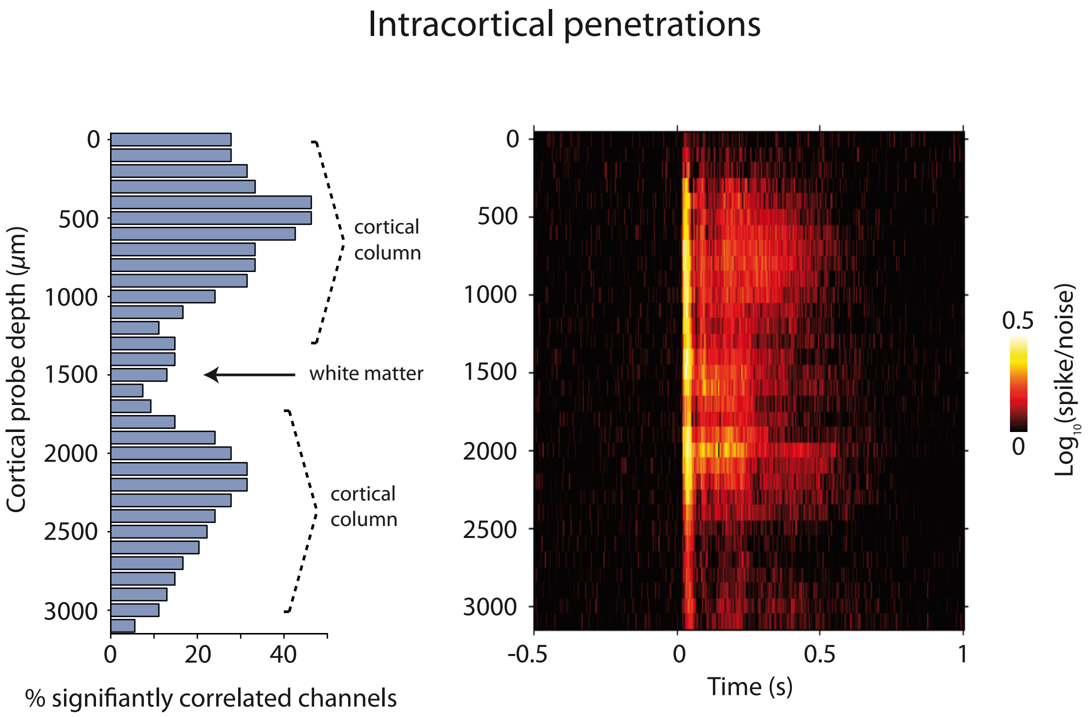

Figure S5. Cortical depth profile. (**A**) Incidence of channels that are significantly correlated with the SC and a function of cortical depth. Note that amplitude correlation effects display two peaks at 500µm and 2200µm below the cortical surface respectively, reflecting that we usually recorded form two vertically adjacent cortical penetrations separated by white matter. (**B**) Population averaged spike/noise ratio for cortical spiking activity in response to visual flash stimulation.

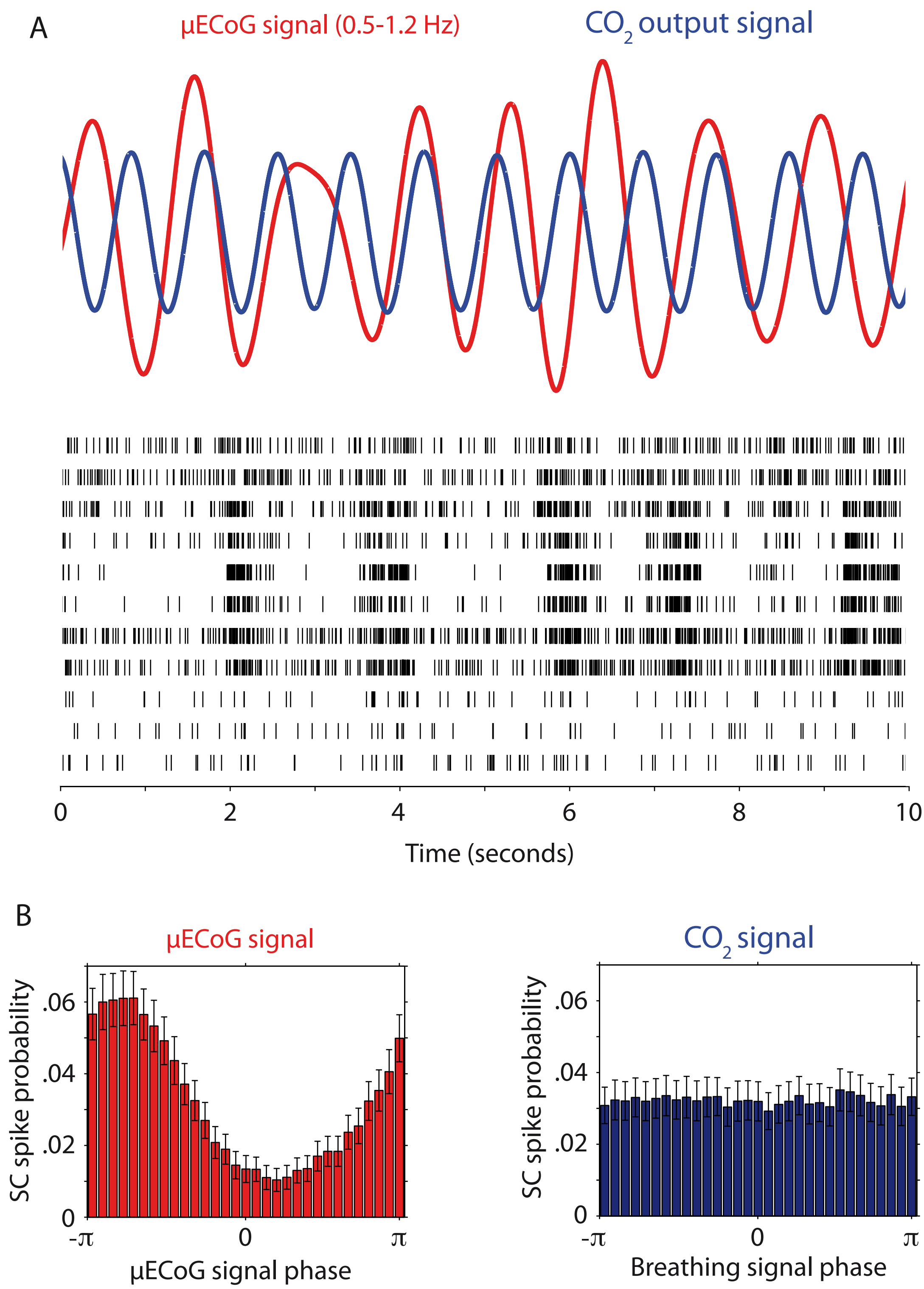

Figure S6. Effects of breathing on coordinated neural activity. (**A**) Filtered μECoG signal time-series plotted along with the simultaneously recorded output of the carbon dioxide breathing monitor. The breathing monitor indirectly tracks any mechanical related brain pulsations caused by ventilation. Note that the endogenous slow brain oscillation and breathing signal appear entirely unrelated. (**B**) Spike-phase histograms computed using SC spiking activity and the phase of μECoG (left) and breathing (right) signals. Note that SC spiking activity is strongly locked to the phase of the endogenous physiological oscillation, and displays no temporal dependency on breathing.

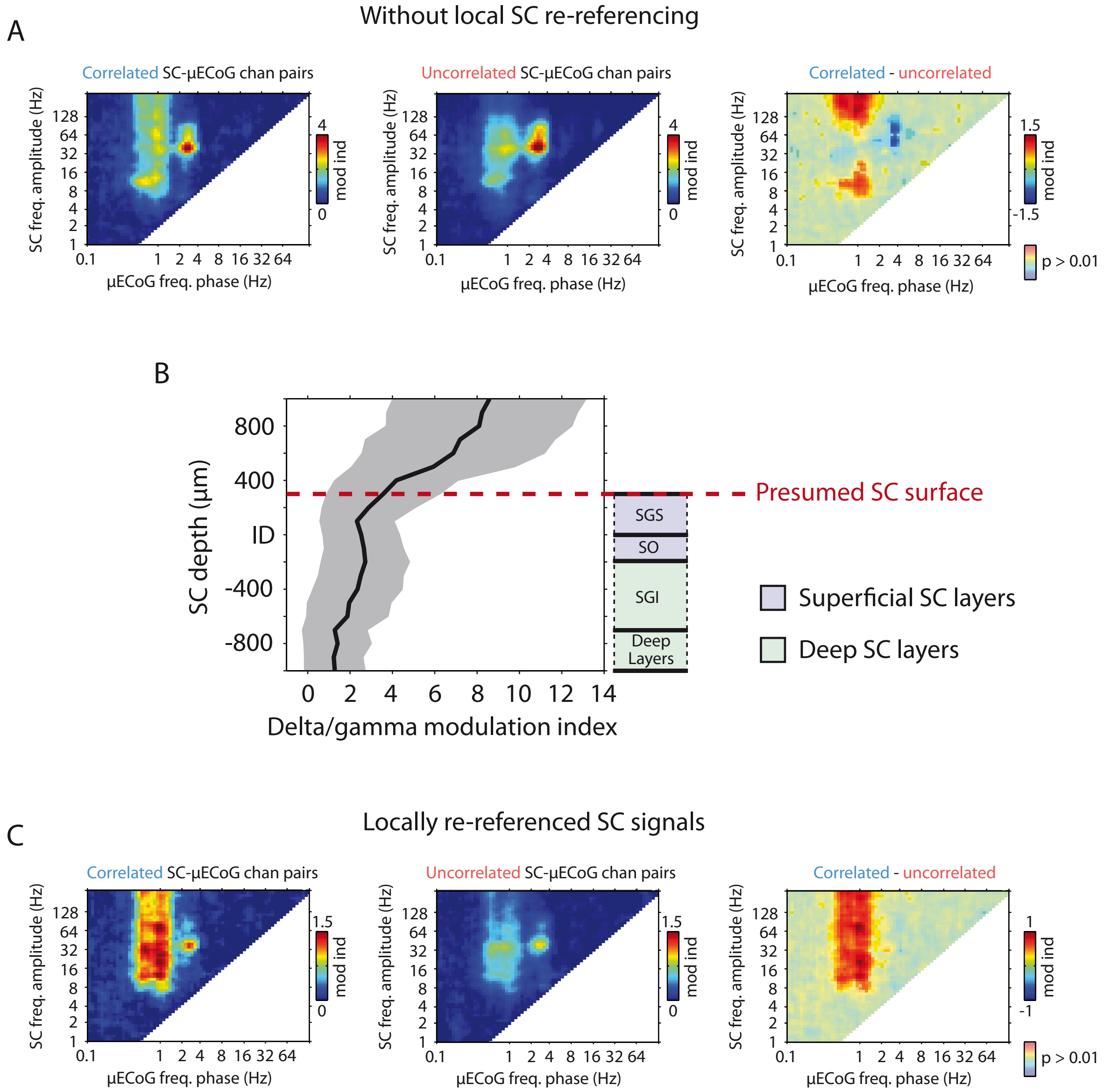

Figure S7. Cross frequency coupling spectra and locally re-referenced signals. (**A**) Population averaged cross-frequency phase amplitude coupling spectra for power correlated (left) and uncorrelated (middle) SC-µECoG channel pairs. The difference between correlated and uncorrelated channel pairs is plotted on the right ($p < 0.01$, Bonferroni corrected). Note the significant locking of spindle and high frequency activity to the phase of slow cortical oscillations. In addition, both correlated and uncorrelated channel pairs display very strong cross-frequency coupling between cortical delta phase and SC gamma activity. (**B**) Population average strength of cortico-tectal delta/gamma phase amplitude coupling as a function of SC depth. Note that the strength of delta/gamma coupling drastically increases for recording contacts that are presumed to be located superficial to the SC. This result suggests that observed delta/gamma coupling may in fact be due to volume conduction from the brain structure directly overlying the SC. (**C**) Results of the same analysis as performed in A, however following the local re-referencing of SC signals. Note that the strong delta/gamma cross-frequency coupling present in **A** is now weakened or absent.

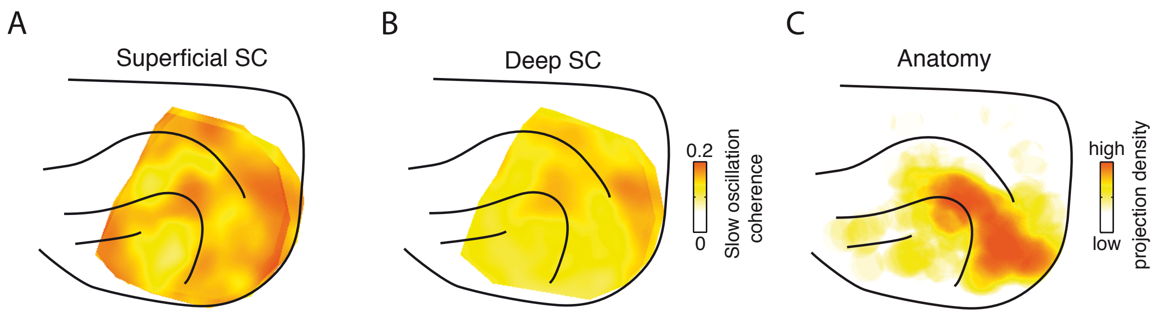

Figure S8. Spatial maps of slow oscillation coherence. (**A**) Population averaged slow oscillation coherence topography for superficial SC recording sites. (**B**) Population averaged slow oscillation coherence topography for deep SC recording sites. (**C**) Plot of the density of tectally projecting neurons across the cortical surface. Data were adapted with permission from *(13)*.